

Purdue University

Purdue e-Pubs

International Refrigeration and Air Conditioning
Conference

School of Mechanical Engineering

2021

External Water Subcooling To Improve The Performance Of A CO2 Heat Pump For Water Heating That Uses Greywater As Heat Source

Ramón A. Otón-Martínez

Universidad Politécnica de Cartagena, Spain

Fernando Illán-Gómez

Universidad Politécnica de Cartagena, Spain, fernando.illan@upct.es

José Ramón García-Cascales

Universidad Politécnica de Cartagena, Spain

F. Javier Sánchez-Velasco

Universidad Politécnica de Cartagena, Spain

Víctor Sena-Cuevas

Universidad Politécnica de Cartagena, Spain

Follow this and additional works at: <https://docs.lib.purdue.edu/iracc>

Otón-Martínez, Ramón A.; Illán-Gómez, Fernando; García-Cascales, José Ramón; Sánchez-Velasco, F. Javier; and Sena-Cuevas, Víctor, "External Water Subcooling To Improve The Performance Of A CO2 Heat Pump For Water Heating That Uses Greywater As Heat Source" (2021). *International Refrigeration and Air Conditioning Conference*. Paper 2143.
<https://docs.lib.purdue.edu/iracc/2143>

This document has been made available through Purdue e-Pubs, a service of the Purdue University Libraries. Please contact epubs@purdue.edu for additional information. Complete proceedings may be acquired in print and on CD-ROM directly from the Ray W. Herrick Laboratories at <https://engineering.purdue.edu/Herrick/Events/orderlit.html>

External water subcooling to improve the performance of a CO₂ heat pump for water heating that uses greywater as heat source

Ramón A. OTÓN-MARTÍNEZ², Fernando ILLÁN-GÓMEZ^{1*}, José Ramón GARCÍA-CASCALES¹, F. Javier SÁNCHEZ-VELASCO¹, Víctor SENA-CUEVAS¹

¹Dep. Ingeniería Térmica y de Fluidos, ETSII, Universidad Politécnica de Cartagena, Cartagena, Murcia, Spain

²Dep. de Ingeniería y Técnicas Aplicadas, Centro Universitario de la Defensa (AGA) San Javier, Murcia, Spain,

* fernando.illan@upct.es

ABSTRACT

The use of CO₂ heat pumps for water heating combined with energy recovery from greywater is a promising technology that can help to improve the efficiency of both domestic hot water (DHW) generation and space heating. A key aspect to keep in mind during the design of any CO₂ refrigeration or heat pump system is the fact that the optimal gas cooler pressure in a transcritical CO₂ cycle is mainly dependent on the refrigerant temperature at the gas cooler outlet. In space heating applications as well as DHW generation, operating conditions require high temperatures of refrigerant at the gas cooler outlet. That can lead to very high optimal pressures, in some cases, even higher than the maximum pressure of the system. The use of a subcooler fed by the same greywater used in the evaporator can help to reduce the optimal pressure and improve the efficiency of the system. When the greywater passes first through the subcooler, the evaporation temperature can be increased while the optimal pressure is reduced. When the greywater passes first through the evaporator, the evaporation temperature remains constant, but the refrigerant temperature at the gas cooler outlet can be reduced to a lower value. So, the order in which the water flows through subcooler and evaporator can affect the system's efficiency and the best control strategy will depend on the operating conditions. First, a numerical model is used to model an experimental facility and model results are compared to some preliminary experimental results. Finally, this contribution analyses the influence that the greywater conditions (temperature, mass flow rate and flow order), as well as the subcooler efficiency have in the system's efficiency depending on the operating conditions (DHW generation or space heating) in order to establish the control strategy that optimizes the system's performance.

1. INTRODUCTION

One of today's high-efficiency alternatives for DHW generation and for space heating is the use of water-water heat pumps. Numerous companies currently market these systems, based on hydrofluorocarbon (HFC) refrigerants. Against the use of HFCs with a big global warming potential (GWP), as much as 1430 (R134a) or 3920 (R404a), international regulations applicable to refrigeration and heating equipment are exhibiting a trend whereby, refrigerants with higher GWP will be progressively discarded and replaced by other options with less environmental implications. At the European level, for example, Regulation (EU) No 517/2014 on fluorinated greenhouse gases contemplated placing on the market prohibitions on HFCs with GWP of 2500 or more, by January 2020, and HFCs with GWP of 150 or more, by January 2022. With these perspectives, the use of CO₂ (R744), a natural fluid, which is neither toxic nor flammable, GWP of 1 and ODP equal to zero, has proven to be an interesting alternative for the future (Nekså *et al.*, 2010).

CO₂ transcritical heat pumps provide high coefficient of performance (COP) for a high temperature lift of water at the gas cooler (around 30-40°C) and a low inlet temperature of the water to be heated. In fact, for those conditions, COP can be higher than that of conventional heat pumps (Austin and Sumathy, 2011). However, the temperature of the water that needs to be heated must be low enough. When the CO₂ is not cooled far enough due to inlet water at gas cooler, as usual in space heating systems, the efficiency of the system will decrease.

Transcritical CO₂ heat pumps work with high refrigerant pressures in the gas cooler. Above 31°C, CO₂ is transcritical, and it is usual that optimal pressure for CO₂ heat pumps is above 100 bar. This is a key aspect to keep in mind during the design of any CO₂ refrigeration or heat pump system and, moreover, considering that optimal gas-cooler pressure in a transcritical CO₂ cycle is mainly dependent on the refrigerant temperature at the gas cooler outlet (Chen and Gu, 2005). In space heating applications the temperature of the water at the gas cooler inlet varies typically around 40 and 55°C, depending on the design of the system (medium to very high temperature, according to the European standard EN 14511). A similar situation occurs in DHW generation, when the temperature of the water in the storage tank approaches set points around 60°C or even higher. In those conditions, the temperature of the refrigerant at the gas cooler outlet can lead to a very high optimal pressure that, in some cases, can be higher than the maximum pressure of the system. In fact, working with high pressures makes heat pump equipment more expensive, which sometimes must be oversized to safely withstand the required pressures. If the maximum pressure limitation forces the installation to work at a pressure set-point lower than the optimum, the COP would be reduced.

In order to reduce the optimal pressure and improve the efficiency of the system, an intermediate heat exchanger, fed by the same water used in the evaporator, can be installed as a subcooler. The order in which the water flows through the subcooler and evaporator can affect the system's efficiency and the best control strategy will depend on the operating conditions. When the greywater passes first through the subcooler, the evaporation temperature can be increased, while the optimal pressure is reduced. When the greywater passes first through the evaporator, the evaporation temperature remains constant, but the refrigerant temperature at the gas cooler outlet can be reduced to a lower value.

The main objective of this work is to analyze the effectiveness of the subcooler working with the cold water of the evaporator. To that end, a mixed methodology based on experimental observations and numerical simulations has been used. First, the experimental installation that has been used in the study will be presented. Likewise, the optimal pressure of the installation is shown, whose expression has been found by means of a regression procedure based on experimental data. The installation has been modeled using numerical expressions, which are presented later in the document, which have been programmed in TRNSYS. Next, the numerical model is used to establish the control strategy that optimizes the performance of the system, depending on the order in which the water flows through the subcooler, the operating set-point conditions, and the influence of the greywater temperature.

2. NUMERICAL MODEL FOR THE EXPERIMENTAL SYSTEM

The water-water heat pump used for the experimental study is a transcritical heat pump, which works with R744 refrigerant and has been dimensioned for a heating capacity of 8 kW. The installation, whose scheme is shown in Figure 1, was installed in the laboratories of Universidad Politécnica de Cartagena. The different components selected to form the heat pump are gathered in Table 1. A group of experiments have been carried out at the system where different operating points have been tested (García-Cascales *et al.*, 2019).

Table 1: Components of the experimental heat pump (manufacturer and model).

Equipment	Manufacturer	Model	Tech. info
Compressor	Dorin	CD300H	$\dot{V} = 1.46 \text{ m}^3/\text{h}$
Evaporator	Swep	B8Tx26P	$A=0.552 \text{ m}^2$
Gas cooler	Swep	B16x34P	$A=1.31 \text{ m}^2$
Liquid to vapour heat exchanger	Swep	B17x4P	$A=0.082 \text{ m}^2$
Back pressure expansion valve	Carel	E2V11CS100	$K_v=0.042 \text{ m}^3/\text{h}$
Thermostatic expansion valve	Carel	E2V24CS100	$K_v=0.18 \text{ m}^3/\text{h}$

Table 2: Adjustment coefficients for compressor behavior curves.

	C ₁	C ₂	C ₃	C ₄	C ₅	C ₆	C ₇	C ₈	C ₉	C ₁₀
\dot{m}	0.004681	-0.002017	0.001428	$-3.2 \cdot 10^{-6}$	$8.45 \cdot 10^{-5}$	$-2.45 \cdot 10^{-5}$	$4.28 \cdot 10^{-7}$	$1.68 \cdot 10^{-7}$	$-5.66 \cdot 10^{-7}$	$1.23 \cdot 10^{-7}$
\dot{W}	966.304	-101.626	-23.414	-0.10299	1.71622	0.64412	-0.021845	-0.005984	-0.005546	-0.003224

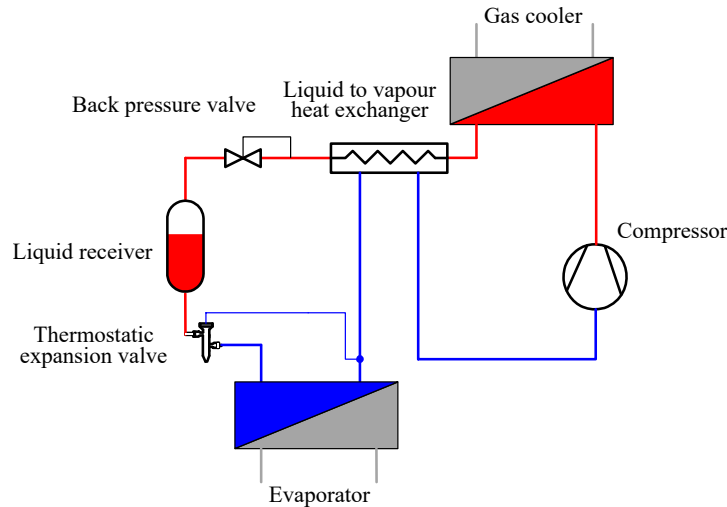


Figure 1: Schematic view of the water-water heat pump.

The behavior on operation of the different components of the experimental heat pump has been modeled by means of numerical expressions, some obtained by means of the manufacturer's data sheets, and others developed from the experimental observation through laboratory tests.

First, the input variables and the possible output variables of each component are identified for the modeling. Discharge pressure in bar (P_c) and evaporation temperature in Celsius (T_0) are the input variables of the compressor (Dorin CD 300H, with a power rating of 2.2 kW, working at output pressure of 90 bar, gas cooler temperature of 45°C, and evaporation temperature of 5°C). The expressions provided by the manufacturer have been corrected, so that mass flow rate (kg/s) and power (W) can be computed as:

$$\begin{aligned} m_r &= C_1 + \left(\frac{\rho_a}{\rho_r}\right) \cdot [C_2 \cdot T_0 + C_3 \cdot p_c + C_4 \cdot T_0^2 + C_5 \cdot T_0 \cdot p_c + C_6 \cdot p_c^2 + C_7 \cdot T_0^3 + C_8 \cdot p_c \cdot T_0^2 + C_9 \cdot T_0 \cdot p_c^2 + C_{10} \cdot p_c^3] \\ W_r &= C_1 + \left(\frac{\rho_a}{\rho_r}\right) \cdot [C_2 \cdot T_0 + C_3 \cdot p_c + C_4 \cdot T_0^2 + C_5 \cdot T_0 \cdot p_c + C_6 \cdot p_c^2 + C_7 \cdot T_0^3 + C_8 \cdot p_c \cdot T_0^2 + C_9 \cdot T_0 \cdot p_c^2 + C_{10} \cdot p_c^3] \end{aligned} \quad (1)$$

where ρ_r is the density of the refrigerant at rated conditions, ρ_a is the actual density at compressor suction, and the adjustment coefficients C_i are those shown in Table 2. And, for the evaporator, enthalpies of inlet fluids, as well as pressure of the secondary fluid at inlet, superheating temperature (ΔT_s) and mass flow rates of both fluids, are used as input variables. The numerical approach for the evaporator considers discretization of each stream: the line where phase change takes places (two-phase part) is divided on N elements of equal vapor quality, while the single-phase part is discretized on N elements with constant temperature.

Inlet pressure of refrigerant, p_{ri} , is calculated by an iterative algorithm by means of a calculated pressure drop. At first iteration, we consider $p_{ri} = (p_{low} + p_{high})/2$, where p_{low} is the saturation pressure at the inlet temperature of secondary fluid, and p_{high} is an arbitrary value. In later iterations, pressure drop is evaluated and used to calculate again outlet pressure, enthalpy and, then, heat exchanged at each cell. If the heat absorbed by the refrigerant is the same as that given by the secondary fluid, the temperatures and enthalpies of the secondary fluid at the different elements can be calculated. Finally, heat transfer coefficients are evaluated from correlations as well as heat transfer surface, A_{calc} , which is compared to the actual area, A_0 , and used as a convergence criterion as:

$$\begin{aligned} p_{high} &= p_{ri} & \text{if } A_0 > A_{calc} \\ p_{low} &= p_{ri} & \text{if } A_0 < A_{calc} \end{aligned} \quad (2)$$

The other two exchangers (the gas cooler and the liquid-vapor exchanger) are single phase, for which the input variables are the mass flow rates of both flows, the inlet pressures and enthalpies. Also, for these components, an iterative procedure is used in which the exchanger is divided into N elements with the same heat exchanged. In the first iteration, an initial value is taken for the inlet temperature, which consists of the arithmetic average between the inlet temperature of the hot flow and the inlet temperature of the cold flow. This allows to compute enthalpy as: $h_{ri} =$

$(h_{low} + h_{high})/2$. With this initial value, the enthalpy of the outlet hot fluid is evaluated. For each element on refrigerant line, pressure drop, and enthalpy are calculated and, then, equally with the secondary fluid. Heat transfer coefficients and calculated surface, A_{calc} , are determined. The convergence criterion is applied then for enthalpies:

$$\begin{aligned} h_{high} &= h_{ri} & \text{if } A_0 < A_{calc} \\ h_{low} &= h_{ri} & \text{if } A_0 > A_{calc} \end{aligned} \quad (3)$$

The calculation methodology used for heat exchangers precisely relies on the proper evaluation of the heat transfer coefficient and pressure drop at each element. A correlation by Bogaert and Bölcs (1995) is used for single phase heat transfer coefficient, and a correlation by Chisholm (1967) is used for pressure drop also for single phase. For the evaluation of two-phase flow pressure drop, a correlation derived by colleagues from the Technical University of Valencia has been used (García-Cascales *et al.*, 2019).

The back-pressure valve and the thermostatic expansion valve just give the same outlet enthalpy they receive as input. Regarding the tank (liquid receiver), mass flow rate, pressure and enthalpy at the inlet are the input variables. Outlet mass flow rates and enthalpies are determined by mass and energy balances at the tank.

4. OPTIMAL HEAT REJECTION PRESSURE

Through an analysis procedure (Illán-Gómez *et al.*, 2021) based on multiple-variable regression, it is known that the optimum working pressure of refrigerant in the gas cooler, $P_{gc,opt}$, can be calculated (in bar) based on the refrigerant outlet temperature in the gas cooler $T_{gc,out}$, temperature of evaporation T_{evap} and inlet temperature at compressor $T_{c,in}$ (all in °C):

$$\begin{aligned} P_{gc,opt} &= \min(140; 11.047 + 2.2756 \cdot T_{gc,out} + 0.047279 \cdot T_{evap} - 0.20814 \cdot T_{c,in}) & \text{if } T_{c,in} < 140^{\circ}\text{C} \\ P_{gc,opt} &= \min(140; 140.74 + 0.031555 \cdot T_{gc,out} + 2.7227 \cdot T_{evap} - 1.0086 \cdot T_{c,in}) & \text{if } T_{c,in} \geq 140^{\circ}\text{C} \end{aligned} \quad (4)$$

The expressions for the optimal pressure are simple linear correlations, but they give accurate results in the range 80 – 140 bar. A maximum value of 140 bar is set, to avoid undesired overpressure values that might damage some components. Indeed, the optimum pressure values given by Eq. 4 are considerably high. For a typical temperature value for high temperature water heating (60°C), optimal pressure would be around the limit of 140 bar. That is a high value, if we consider that many R744 heat pump manufacturers limit the pressure to values around 120 bar. In fact, the use of lower pressures generally reduces the cost of the components of the system, and although a gas cooler pressure under the optimum could reduce the COP, it could also decrease the cost of installation.

5. EXPERIMENTS AND MODEL VALIDATION

Making use of the installation according to the configuration in Figure 1, multiple cases with different operating points have been tested. In particular, a total of ten cases are presented with the conditions that are summarized in Table 3.

Table 3: Summary of the working conditions for the experiments in the transcritical heat pump.

Case	Higher pressure (bar)	Pressure at liquid receiver (bar)	Evaporator secondary fluid Temperature (°C)		Gas Cooler water Temperature (°C)	
			In	Out	In	Out
01	80	60	10	7	30	35
02	80	60	15	N	N	35
03	80	61	20	N	N	35
04	80	61	25	N	N	35
05	85	67	10	7	35	40
06	85	66	15	N	N	40
07	85	66	20	N	N	40
08	85	66	25	N	N	40
09	75	70	10	7	30	35
10	85	57	10	7	30	35

Experiments were designed following the indications of the UNE-EN 14511 standard. The objective of the tests is to cover a wide range of operating conditions, which could be required for a heat pump of these characteristics working to produce domestic hot water. For a maximum pressure between 75 and 85 bar, the water inlet temperatures in the evaporator secondary fluid range between 10 and 25 °C. The inlet water temperature in the gas cooler varies between 30 and 40°C, while the outlet temperature is between 35 and 45°C. The variables marked as “N” are not imposed, but only monitored.

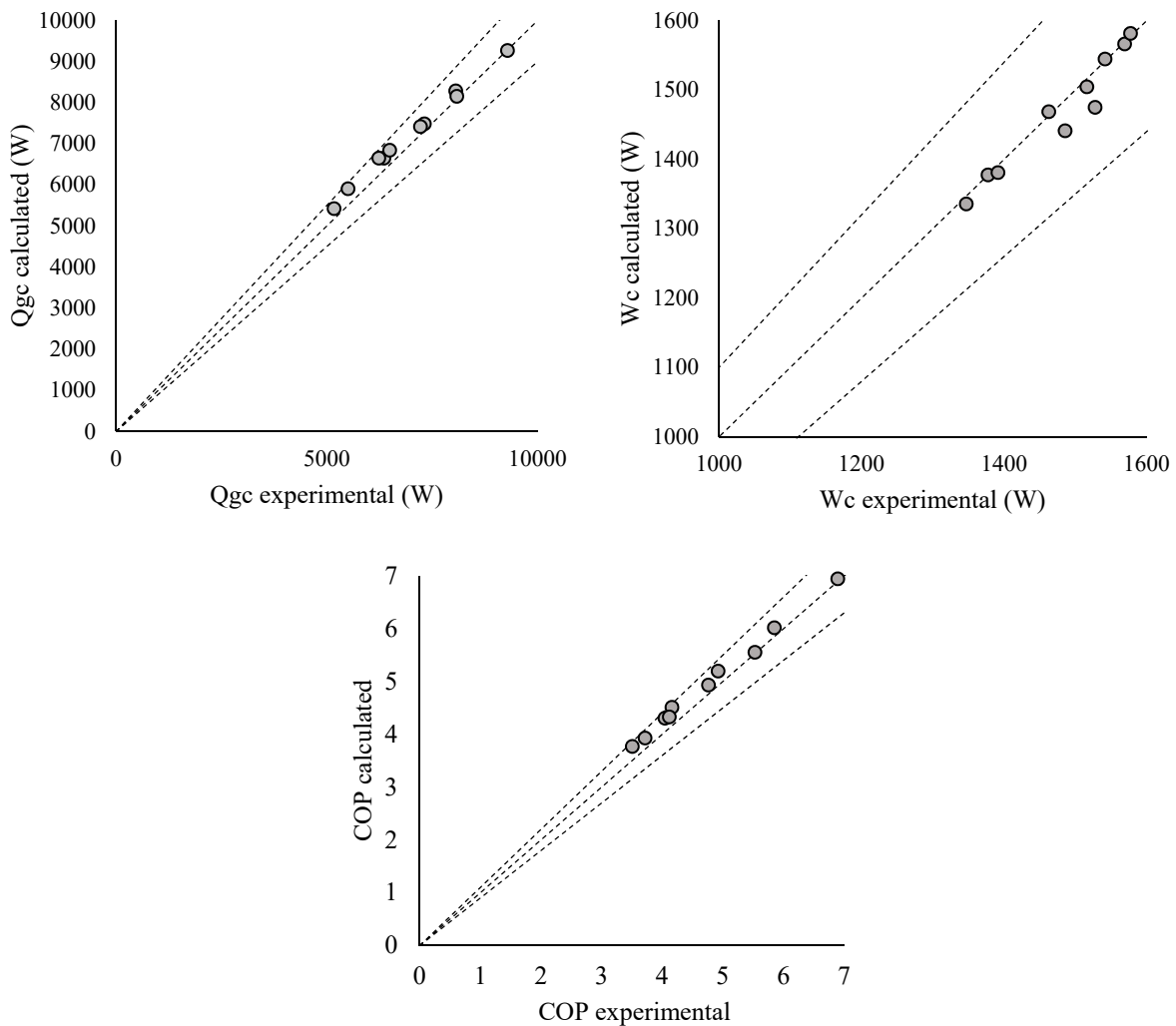


Figure 2: Numerical (TRNSYS calculated) vs. experimental results for the CO₂ heat pump.

In the first test (case 01), a reference flow rate of refrigerant is set, that complies with the fact that the secondary fluid at the evaporator enters at 10°C and leaves at 7°C, while in the gas cooler the secondary water enters at 30°C and leaves at 35°C. This flow rate is set for the following three cases, in which the inlet temperature of the secondary water in the evaporator varies. The same is repeated in the following four cases, starting from a base case with temperatures of 10°C / 7°C in the evaporator and 35°C / 40°C in the gas cooler. The following cases are pressure variations in the liquid receiver and the gas cooler temperatures. These experiments constitute a database destined for the validation of the numerical models that were presented in section 2, and that have been implemented in a TRNSYS 17 model, following the scheme of Figure 1. For this, TRNSYS needs a series of input data, from which the software simulates a transient that converges to the stationary operating point of the installation, equivalent to the case studied

experimentally. In this way, it is possible to obtain the remaining output data from the simulation software and compare it with the values of these experimentally measured variables.

For the model input, there are fourteen needed variables: compressor outlet pressure, superheating temperature in evaporator, inlet temperature, pressure and mass flow rate of the secondary fluid in the evaporator, inlet pressure of refrigerant in gas cooler, inlet temperature, pressure and mass flow rate of the secondary fluid in the gas cooler, pressure at vessel, refrigerant mass flow rate at the compressor, inlet pressure and enthalpy at the compressor and outlet enthalpy in thermostatic expansion valve. These variables are provided to the software as input from the experimental data base.

The output variables can be represented as in Figure 2, so that numerical versus experimental comparisons can be done. In particular, the heat released in the gas cooler (Q_{gc}), the compressor power (W_c) and COP are presented. Dashed lines represent $\pm 10\%$ relative error for each magnitude compared. As observed, relative error between calculated and experimental always lies within this interval. Results for compressor power are particularly good.

6. NUMERICAL RESULTS ON HEAT PUMP MODIFIED CONFIGURATIONS

The transcritical CO₂ heat pump represented in Figure 1, which has been experimentally tested, provides good COP values, in the range of 3.7 to 6.9, for the entire range of points tested. All the tests, except case 5, present an experimental COP greater than 4.0. The three points with the best COP are cases 3, 4 and 8, all with COP higher than 5.5, which is logical, since those are the cases in which the temperature of inlet water in the evaporator is higher. However, if we increased the predetermined value of the water outlet temperature in the gas cooler, which is the temperature of the water that is sent to the hot water and heating circuit, we would observe two simultaneous effects: (i) the displacement of the thermodynamic cycle towards the highest part of the saturation curve, and (ii) the drastic reduction of the COP.

Due to the critical temperature of CO₂ at 31.03°C, when trying to set moderately-high hot water delivery temperatures, the transcritical CO₂ cycle shifts to the right in the $p - h$ diagram, so that much of the cycle is carried out outside the saturation zone, in gaseous state. Besides, the system tends to adjust to the optimum pressure, as described in Section 4, what increases the working pressure. That in turn shifts the cycle up on the $p - h$ diagram. Therefore, working conditions are achieved with a significantly decreased COP.

In addition, the increase in pressure has its consequences from the point of view of the design of the installation. Working with such high pressures makes elements and materials more expensive, as the design must guarantee the safety and durability of the system in such working conditions. That is the reason why R744 heat pump manufacturers usually limit the maximum working pressure to values around 120 bar, even at the risk of reducing the COP by moving away from the optimum working pressure. In order to achieve high discharge hot water temperatures, in those cases, heat pump units can incorporate electric heaters, which come into operation in cases where the thermodynamic cycle cannot meet the setpoint temperature.

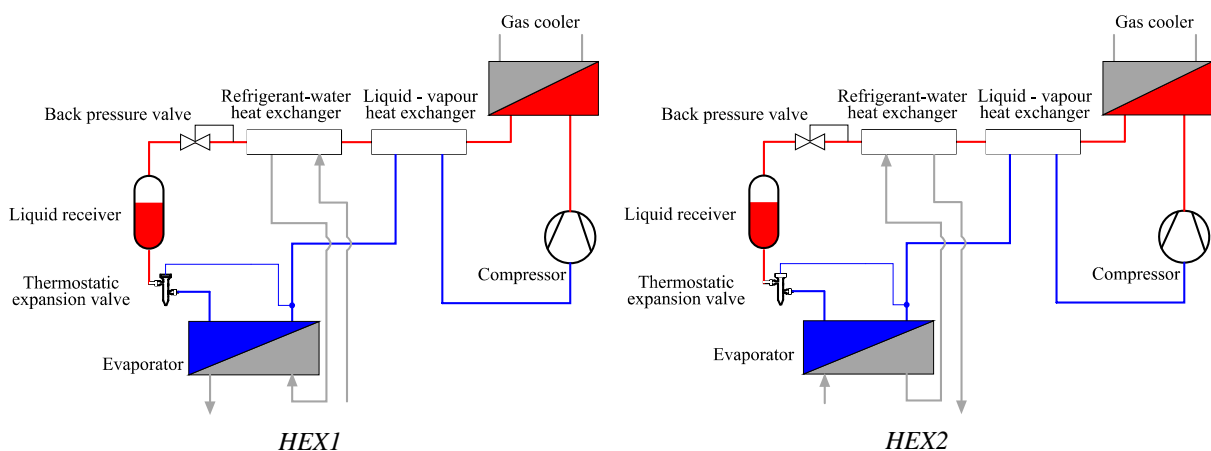


Figure 3: Two new heat-pump configurations with intermediate liquid-liquid heat exchanger.

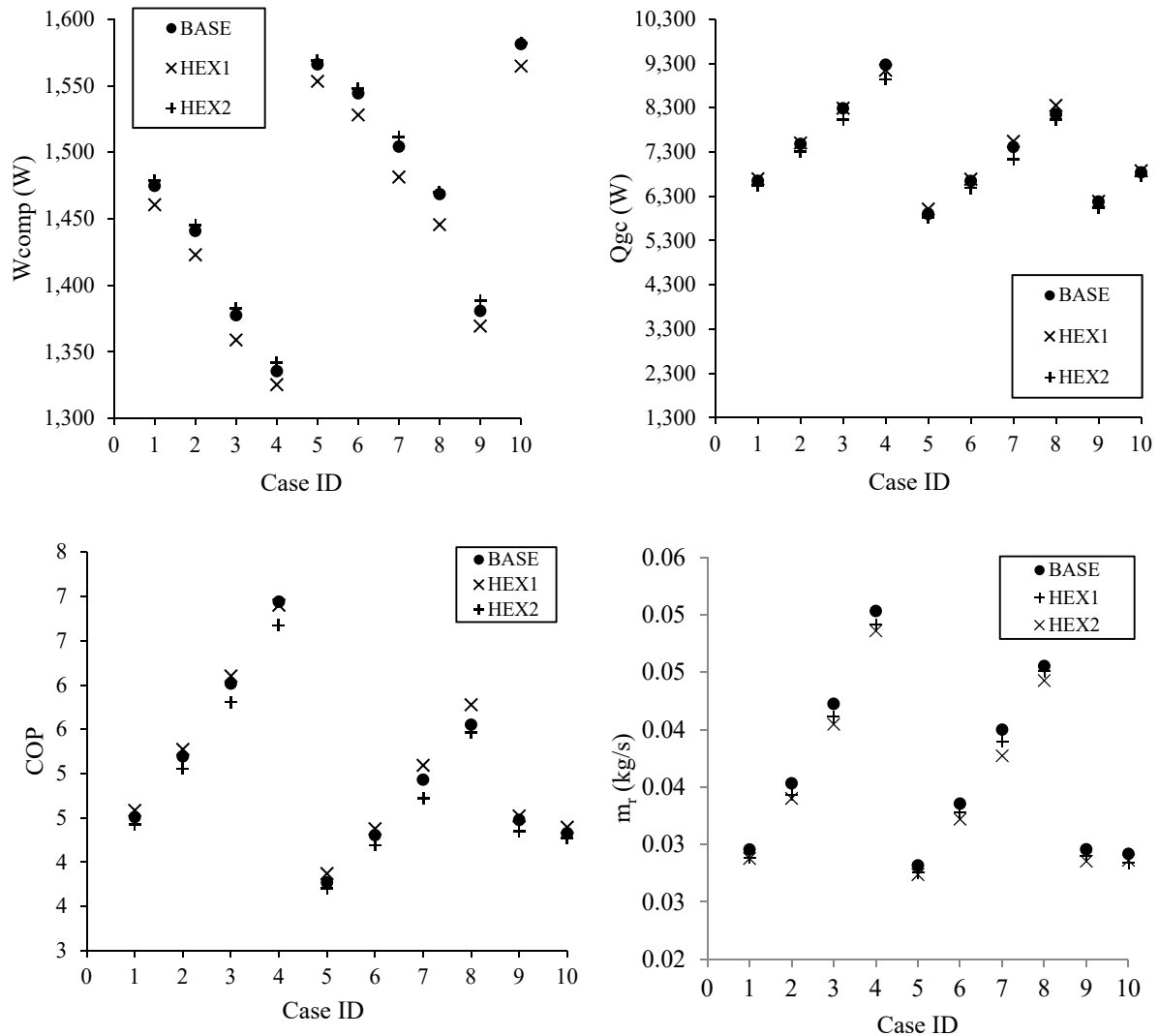


Figure 4: Numerical results for the CO₂ heat pump (*BASE*) and two new configurations with intermediate heat exchanger (*HEX1* and *HEX2*).

In order to avoid the installation of these electric heaters, which notably increase the power consumption of the system, two different configurations of the same alternative are proposed in this paper: the installation of an intermediate heat exchanger, between the cold water of the evaporator and the refrigerant leaving the liquid-to-vapor heat exchanger. The model selected is a SWEP B18Hx20, with 20 plates, a total heat transfer surface of 0.738 m², which, according to the manufacturer's data sheet, shows a heat transfer capacity of 9.6 kW, working with CO₂ (0.05 kg/s at 55°C, $NTU = 4.0$) and water (0.37 kg/s at 22°C, $NTU = 0.8$). The inclusion of this new exchanger has the objective of increasing the subcooling of the refrigerant before its entry into the expansion valve. In this way, R744 would enter the evaporator with a somewhat lower vapor quality and would allow the cycle to run even with high setpoint temperatures.

The two proposed configurations, as can be seen in Figure 3, differ in the order of passage of cold water through the exchanger. In the first case, which we will call *HEX1* (Figure 3, left), the cold water first passes through the intermediate exchanger and then through the evaporator. In the second case, which we will refer to as *HEX2* (Figure 3, right), the water first passes through the evaporator and, at its outlet, is introduced into the new exchanger. Both configurations have been studied with TRNSYS, making use of the models that have been presented in previous sections and whose results were validated with experimental data. In this way, we can evaluate the goodness of each

option before putting it into practice in the installation. Hereinafter, the results obtained with the initial configuration of Figure 1 will be called as *BASE* case.

To illustrate the effect the intermediate heat exchanger has on the performance of the cycle, for each of the studied configurations, the results by TRNSYS have been represented in Figure 4, in particular the power of the compressor (top, left), the heat released in the gas cooler (top, right), COP (bottom, left) and the mass flow of refrigerant in the intermediate exchanger (bottom, right). As can be seen, including the exchanger in the *HEX1* configuration produces an appreciable drop in compressor power. However, with the *HEX2* configuration the effect is opposite and the required power increases. From the point of view of the heating power, the variations are so small that it can be considered constant for the three options. As a combination of the two previous parameters, the $COP = \dot{Q}_{gc}/\dot{W}_c$ shows an improvement for the *HEX1* case and slightly worsens for the *HEX2* case. It is extracted from these results that including an intermediate exchanger in the way of *HEX1* would have a beneficial effect on the cycle and would be recommended from the point of view of energy consumption and efficiency.

On the other hand, it could be questioned, from the economic point of view, whether it compensates the expense of including a new component in the installation, whose effect in terms of improving efficiency, although positive, is limited. The answer is found in the data discussed at the beginning of this section, as well as in the section about optimal pressure. Indeed, for DHW applications where a moderate-high water temperature is required, the pressure increase in the CO₂ cycle is considerable. In these cases, the inclusion of the intermediate exchanger is beneficial because it avoids working at too high pressures and, furthermore, by maintaining the COP (or even slightly increasing it), it would not be necessary to use auxiliary electric heaters to meet the temperature set point for water outlet.

6. CONCLUSIONS

The use of transcritical CO₂ water-to-water heat pumps for domestic hot water generation and heating is a promising option, due to the environmental advantages of R744 and the high COP values of these systems, which make them considered within the category of renewable energies. However, its use in domestic applications still poses some challenges that must be addressed, due to the usually high temperature requirements for these applications.

The characteristics of R744, mainly its critical temperature and pressure, influence the high optimum operating pressures of heat pump systems, when working under the conditions set out in this work. Through the mathematical processing of experimental data obtained from the investigational installation that has been described, a multi-variable regression has been carried out and an expression of the optimum pressure of the installation has been found as a function of the working conditions. This optimum pressure is, for operating temperatures around 60°C, higher than the maximum pressure limit usually set by manufacturers.

In order to analyze the installation from a numerical view, with a reliable and validated approach, models have been developed for each of the system components, which have been integrated into a cycle using the TRNSYS software. The numerical results have been contrasted with the results previously obtained in a series of experimental tests, designed from the UNE-EN 14511 standard.

Once we considered the model that has been validated, two new configurations have been proposed for the studied system, consisting of the inclusion of an intermediate heat exchanger to increase the subcooling of the refrigerant. The analysis of the numerical results has allowed to observe that the inclusion of this IHEx (in the case in which the cold water is introduced first to the IHEx and later to the evaporator) produces an appreciable increase of the COP. Although this increase may not be enough to economically justify the exchanger, the possibility of working at high temperatures without compromising performance or maximum pressure would justify this new configuration.

REFERENCES

- [1] Austin, B.T.; Sumathy, K. (2011). Transcritical carbon dioxide heat pump systems: A review. *Renewable and Sustainable Energy Reviews* 15, 4013–4029.
- [2] Bogaert, R.; Bölcs, A. (1995). Global performance of a prototype brazed plate heat exchanger in a large Reynolds number range. *Experimental Heat Transfer* 8, 293–311.
- [3] Chen, Y.; Gu, J. (2005). The optimum high pressure for CO₂ transcritical refrigeration systems with internal heat exchangers. *International Journal of Refrigeration*, 28, 1238–1249.

- [4] Chisholm, D. (1967). A Theoretical Basis for the Lockhart-Martinelli Correlation for Two-Phase Flow. *International Journal of Heat and Mass Transfer* 10, 1767–1778.
- [5] García-Cascales, J.R.; Illán-Gómez, F.; Sánchez-Velasco, F.J.; Sena-Cuevas, V.F.; Molina-Valverde, R. (2019) Characterisation of the behaviour of a CO₂ water/water heat pump for hot water generation. *25th International Congress of Refrigeration, Montreal, Canada*.
- [6] Illán-Gómez, F.; Sena-Cuevas, V.; García-Cascales, J.R.; Velasco F.J.S. (2021). Analysis of the optimal gas cooler pressure of a CO₂ heat pump with gas bypass for hot water generation. *Applied Thermal Engineering*, 182, 116110.
- [7] Nekså, P.; Walnum, H. T.; Hafner, A. (2010) CO₂ - A refrigerant from the past with prospects of being one of the main refrigerants in the future. *9th IIR Gustav Lorentzen Conference 2010 - natural refrigerants – real alternatives, Sydney*.
- [8] UNE-EN 14511, *Air conditioners, liquid chilling packages and heat pumps with electrically driven compressors for space heating and cooling - Part 1: Terms, definitions and classification*, (Equiv. EN 14511-1:2013) UNE. (2014).
- [9] UNE-EN 14511, *Air conditioners, liquid chilling packages and heat pumps with electrically driven compressors for space heating and cooling - Part 3: Test methods*, (Equiv. EN 14511-1:2013) UNE. (2014).

ACKNOWLEDGEMENTS

This work has been financed by project ENE2017-83665-C2-2-P financed by the Spanish Ministry of Economy, Industry and Competitiveness, and the European Regional Development Fund; and a doctoral scholarship from the Ministry of Higher Education from Dominican Republic (MESCYT) with the contract number BIM-0010-2018.